Available online at www.sciencedirect.com
SCIENCE DIRECT®
ELSEVIER
Journal of Crystal Growth 263 (2004) 125–131
JOURNAL OF CRYSTAL GROWTH
www.elsevier.com/locate/jcrysgro

Study on polycrystallization in bulk $In_xGa_{1-x}As$ using micro-Raman and photoluminescence

M.R. Islam[a,*], P. Verma[b], M. Yamada[a]

[a] *Department of Electronics and Information Science, Kyoto Institute of Technology, Matsugasaki, Sakyo-ku, Kyoto 606-8585, Japan*
[b] *Venture Laboratory, Kyoto Institute of Technology, Japan*

Received 10 September 2003; accepted 18 November 2003
Communicated by G. Müller

Abstract

Micro-Raman and photoluminescence experiments have been performed to characterize the polycrystalline region in the wafers cut from a bulk $In_xGa_{1-x}As$ crystal, which was found to be initiating from the inner part of the ingot, unlike the usual observation of polycrystallization starting from the peripheral part of an ingot. This indicates the existence of polycrystallization mechanism other than those relating to the boundary effects. The polycrystalline region was found to have a random fluctuation of composition. The possibility of drastic local fluctuation in composition, which can be occurred by convection-induced local supercooling, being the main cause of polycrystallization, is investigated here.

PACS: 81.10.Fq; 78.55.Cr; 78.30.Fs

Keywords: A1. Micro-Raman; A1. Photoluminescence; A1. Polycrystallization; B1. Bulk $In_xGa_{1-x}As$

1. Introduction

Bulk $In_xGa_{1-x}As$ crystal is a promising substrate material for fabricating various optoelectronic devices in the next generation of optical fiber communication systems. By choosing a proper value of composition x, the lattice parameter can be tuned either to match the epilayer, or to develop a controlled strain in the epilayer. In order to fabricate a wide variety of devices on an $In_xGa_{1-x}As$ substrate, it is a basic requirement to have the large size of $In_xGa_{1-x}As$ single crystal with homogeneous composition. In particular, the crystals with $x = 0.3$ are in high demand, because of their usages in various light-emitting and communication devices. However, there are some difficulties in growing a homogeneous $In_{0.3}Ga_{0.7}As$ single crystal, because during the growth process, a high segregation effect, in addition to the normal convection, prevents the In concentration constant at this composition in the melt. This has high potential to cause local supercooling, which seems to be one of the major reasons for compositional inhomogeneity as well as local polycrystallization in the grown crystals. Several growth methods [1–6] have been applied to grow bulk $In_xGa_{1-x}As$ crystals. However, the large size of single crystals with homogeneous composition at $x = 0.3$ could not be obtained. Although Kinoshita

*Corresponding author. fax: +81-75-724-7400.
E-mail address: islam@djedu.kit.ac.jp (M.R. Islam).

0022-0248/$ - see front matter
doi:10.1016/j.jcrysgro.2003.11.085

et al. [6] have recently succeeded to grow a homogeneous single crystal with 20 mm length by the traveling liquidus zone method, its diameter is limited to only 2 mm, which is too small for its practical use as a substrate. On the other hand, Kodama et al. [5] have grown single crystals with the diameter of 15 mm by improving the multi component zone melting (MCZM) method; however, its length is limited to about 4 mm due to polycrystallization. In order to grow the large size of $In_xGa_{1-x}As$ single crystals, it is very important to investigate the mechanism of polycrystallization.

It is usually observed that polycrystallization during growth process starts at the periphery of the sample near the crucible, which is commonly correlated with factors such as temperature gradient [7] and temperature fluctuation [8] at the solid–liquid interface, the growth facets [8], the shape of the interface [9], the purity of raw material and cone angle of the crystal [10]. In the present study, we investigate the polycrystallization in bulk $In_xGa_{1-x}As$ crystal grown by the two-step MCZM method [5]. In this method, the composition of crystal is gradually increased from the GaAs seed to a composition of about $x = 0.3$ in the first step, and then the crystal is grown by keeping the composition constant at this value in the second step. The etching images of wafers sliced perpendicular to the growth direction indicate that the polycrystallization was initiated at a certain growth length from the inner part of the crystal, and then it increased in size along the growth length. This special type of polycrystallization was found to initiate in a few growth experiments in the MCZM method. Therefore, the crystal investigated here should have the existence of polycrystallization mechanism other than those associated with the boundary effects.

In order to understand the possible mechanism of polycrystallization, we have investigated the wafers using micro-Raman and photoluminescence (PL) measurements.

2. Experimental method for polycrystallization investigation

In the present study, we anticipate that polycrystallization occurs due to local fluctuation of composition, which could have been caused by localized supercooling. Further, local fluctuation of composition also develops strain in the sample. Therefore, we need a through characterization of compositional variation, strain and polycrystallization. Both Raman and PL are nondestructive efficient ways to investigate composition, strain and crystallinity of a semiconductor. Shift in optical phonons in Raman spectra originates from the change in composition for unstrained crystals [11]. However, in the presence of strain, phonon positions contain composition-dependent shift as well as strain-induced shift [12,13]. On the other hand, phonon intensities in Raman spectra depend on the crystal orientation, which helps in determining the crystalline qualities. Therefore, Raman scattering is a good characterization technique to determine the composition, residual strain and the presence of polycrystallization. Similarly, both luminescence peak position and intensity in PL spectra depend, respectively, on the composition and crystal orientation [14]. In addition to this, PL is a convenient fast technique for two-dimensional mapping of peak position and integrated intensity, which picture out the compositional variation and crystallinity, respectively, across the entire sample. It should be mentioned here that, at room temperature PL due to the band-to-band transition dominates over other transitions through impurities and so on. Although PL peak energy could be shifted slightly from the band gap energy of materials, PL spectrum is sharp enough to determine composition with high accuracy. By assuming the PL peak energy as band gap energy, the compositions evaluated in various unstrained polycrystalline materials were found to be deviated about 5% with those evaluated by standard chemical analysis method [14]. Therefore, a combination of Raman scattering and PL is best suitable for the crystal under investigation.

3. Experimental procedure

Bulk $In_xGa_{1-x}As$ crystal of 15 mm diameter was grown by the two-step MCZM method [5]. The crystal was cut in two semi-cylindrical pieces along the growth length. The cut surface of one piece was

mechanically polished to evaluate the compositional variation at the centerline along the growth direction of the piece using energy-dispersive X-ray analysis. It was confirmed that the composition gradually increases from $x = 0.05$ to $x \sim 0.3$ from the seed–crystal interface up to a certain distance in the growth direction. The other piece was chemically etched with 90% H_2SO_4:5% H_2O_2:5% H_2O, so as to check the single crystal region by means of etching image. Later, both semi-cylindrical pieces were sliced into wafers perpendicular to the growth length. These wafers were also etched for examining their etching images and were polished for Raman and PL measurements. After certain growth length in increasing composition region, the etching images of wafers indicate the formation of polycrystallization. Therefore, these wafers were considered in the present study, which were obtained from the growth lengths of 19, 20, 21, and 22 mm, and will be referred as wafers A, B, C, and D, respectively, for further discussion.

Raman scattering measurements were made at room temperature using a Ranishaw model 2000 micro-Raman system equipped with an argon-ion laser ($\lambda = 514.5$ nm). The incident light was focused to a spot of about 2 μm on the sample surface with a 50× objective lens and the scattered light was collected by the same objective lens. Typical slit width used was about 100 μm. Low laser power was used to prevent the local heating and optical damages of the sample.

Using a PL mapping system equipped with a 17 mw He–Ne laser and a cooled InGaAs detector, PL measurements were also performed at room temperature. The optical arrangement was similar to that of Raman scattering. The wafers were scanned by computercontrolled XY-translational stages. Peak positions of PL spectra were determined by lineshape fittings.

4. Results and discussions

Fig. 1 shows the etching images of wafers A, B, C, and D. The etching image obtained from the wafer B shows a small dark region within the crystal, which is enclosed by dotted lines to emphasise its position. This region was found to increase in size with increasing the growth length, as seen in the etching images of the wafers C and D. The wafers obtained after the wafer D at longer growth lengths show that this region further increases in size. However, such dark region was not found in the etching image of the wafer A, which is adjacent to the wafer B. Therefore, etching results indicate that the dark region was initiated from the wafer B, and increased in size with growth length. Such dark regions in etching images typically indicate polycrystalline region. In order to confirm this, and to further characterize these regions, the wafers were investigated by Raman scattering and PL measurements.

The first-order Raman spectrum from a ternary compound semiconductor $In_xGa_{1-x}As$ typically shows LO and TO phonons [11,15–17] corresponding to both InAs and GaAs binary parent materials. However, depending upon the crystal orientation and experimental geometry, one of them may be optically forbidden. The frequency positions and appearance of these phonons are strongly influenced by the alloy composition and crystal orientation. Fig. 2 shows some of the Raman spectra, which were measured at a lateral interval of 50 μm from the front surface near and across the dark region of the wafer B. The inset of Fig. 2 shows an enlarged view of the investigated

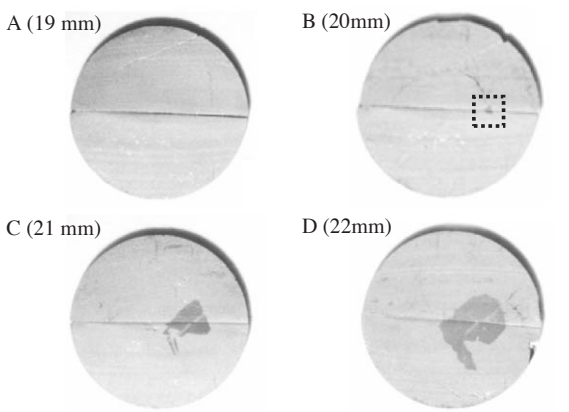

Fig. 1. Etching images of the wafers sliced at the different growth length of the crystal. A small black region shown inside the dotted square was found to increase in size with growth length. The crystallinity in this region appears to be changed with respect to the surrounding.

region. The spectra shown from the top to the bottom in Fig. 2 correspond, respectively, to the points represented by the letters a to j in the inset. It is found that the GaAs-like phonons (TO_{GaAs} and LO_{GaAs}) are stronger than the InAs-like phonons (TO_{InAs} and LO_{InAs}) in Raman spectra due to low In content in the wafer. It is also found that Raman spectra measured in the dark region show random shift in phonons peak positions, where some spectra also show drastic change in intensity ratio between TO_{GaAs} and LO_{GaAs} phonons. Since LO_{GaAs} phonons are stronger in the spectra, we will consider this phonon for further discussion. The exact peak positions of phonons were determined by the best lineshape fitting with Lorentzian components and a proper background.

Fig. 3(a) shows the variation of LO_{GaAs} peak positions and the relative intensity ratio LO_{GaAs}/TO_{GaAs} as a function of distance from the center

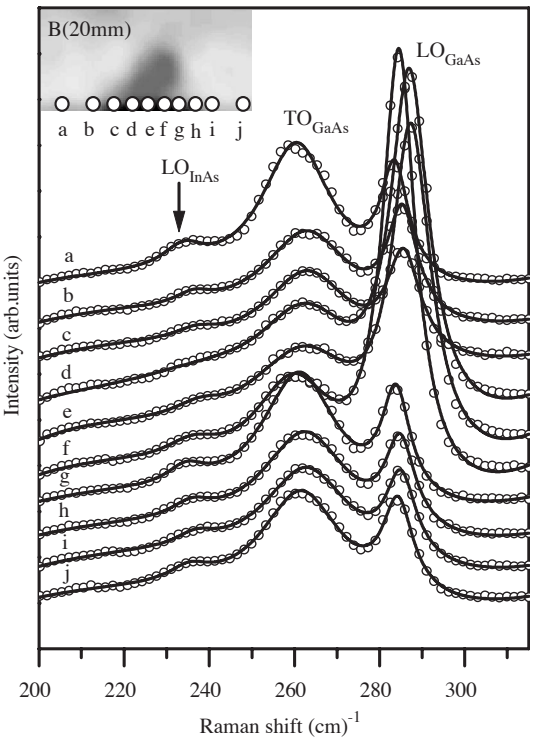

Fig. 2. Raman spectra measured near and in dark region from the front surface of the wafer B corresponding to the measurement points shown in the inset.

of the wafer B. The left and right hand scales in Fig. 3(a) correspond to the LO_{GaAs} peak position and LO_{GaAs}/TO_{GaAs} intensity ratio, respectively. It is found in Fig. 3(a) that LO_{GaAs} peak positions measured in the dark region show random shift in the higher frequency side, with some part (measurement points between d and e) showing a shift as high as 2 to 3 cm^{-1} than the peak positions measured outside the dark region. It is also found that LO_{GaAs} peak positions measured at the right side out of the dark region show a shift of about 0.75 cm^{-1} than the peak positions measured from the left side out of the dark region.

Since etching images indicate that the dark region was initiated from the wafer B, Raman spectra were measured from the side surface of this wafer to investigate its origin. The measurement schematic is shown in the inset of Fig. 3(b). Similar to Fig. 3(a), Fig. 3(b) also shows that the LO_{GaAs} peak positions measured in the dark region were shifted in the higher frequency than those measured outside of the dark region. This indicates that the dark region has lower In content than the outside of the dark region and its amount fluctuates drastically inside the dark region. Further, the position of LO_{GaAs} peaks shown in Figs. 3(a) and (b) indicates that In content decreases from the left to the right side out of the dark region. The random fluctuation of In content in the dark region as well as difference of In content in both sides out of the dark region could occur due to diffusion of In from the nucleation side of the this region. Since compositional inhomogeneity exists in the dark region, the observed Raman peak positions should have the influence of strain.

It is well established that due to the selection rules, the intensity ratio between LO and TO phonons strongly depends on the crystal orientation [15]. The change in phonon intensity in Raman spectra can, in general, be observed only for a significant change in crystal orientation. Fig. 3(a) shows the relative intensity ratio LO_{GaAs}/TO_{GaAs} measured in the dark region from the front surface of the wafer B. Since relative intensity ratio LO_{GaAs}/TO_{GaAs} measured from the points a and j outside of the dark region is the same, the outer region can be considered as

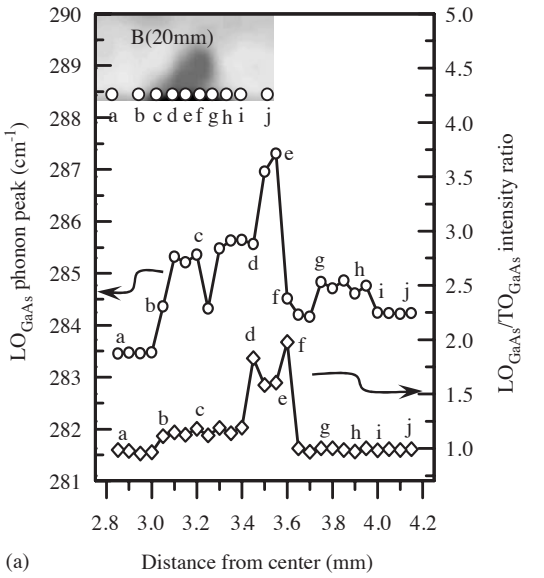

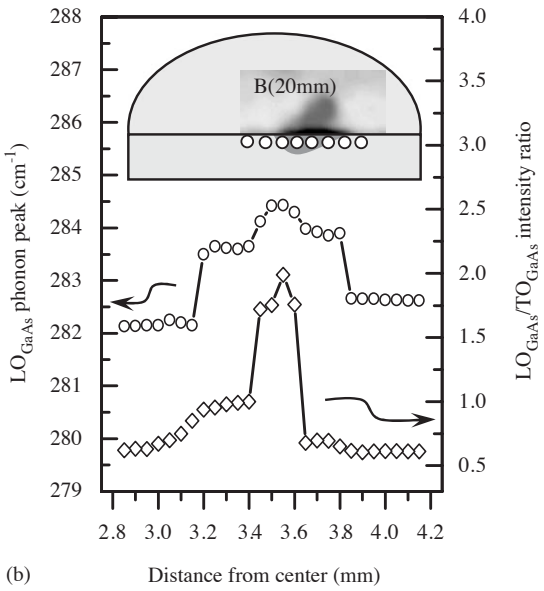

Fig. 3. (a) and (b) LO_{GaAs} phonon peak positions and LO_{GaAs}/TO_{GaAs} intensity ratio measured from the front and side surfaces of the wafer B, where left- and right-hand scales correspond to, respectively, phonon peak positions and relative intensity ratio. The insets show enlarged view of the investigated regions, in which open circles represent some of the measurement points.

single crystal region. However, the slight change in intensity ratio at the boundary of the dark region indicates the beginning of polycrystallization starting from the boundary of the dark region. Inside the dark region, since some small regions (between points d and f) show a significant change in intensity ratio, which is about two times than the out side of the dark region, crystal orientation in these regions has been changed significantly. Thus, it is confirmed that dark region is a polycrystalline region. Similar results are also found from the side surface of the wafer B as shown in Fig. 3(b). However, such a change in intensity of phonons was not found in Raman spectra measured from the wafer A, which indicates polycrystallization was initiated from certain part of the wafer B.

In order to confirm the Raman results, PL experiments were performed in these wafers at a spatial resolution of 20 μm. Figs. 4(a) and (d) show the etching images of the semicircular wafers B and C, respectively, where the scale in millimeter indicates the exact position of the polycrystalline region. Figs. 4(b) and (c) show the PL mapping from the peak wavelengths (composition maps) corresponding to the dotted area shown in Fig. 4(a), from the front and side surfaces of the wafers B, respectively. Figs. 4(e) and (f) show similar results for the wafer C. The PL map shown in Fig. 4(b) shows drastic change in composition near the boundary of the polycrystalline region than the surrounding in agreement with the Raman results. Similar results are also found in Fig. 4(e). It is also observed in Fig. 4(b) that the central part of the polycrystalline region shows slightly higher In content than the boundary of the polycrystalline region. This In-rich part is found to increase in size with increasing growth length as shown in Fig. 4(e). It is also found in Fig. 4(e) that some points inside the polycrystalline region show lower In content, in agreement with the Raman results. It is observed in Fig. 4(c) that the origin of polycrystalline region shows more Ga content, but close to the origin a tiny region shows more In content than the surrounding. This In-rich region is further found to be increased in size in Fig. 4(f). Although the central part of this In-rich region contents more In than near the boundary, some points at the central region show lower In content. Besides the central region, the surrounding of the polycrystalline region contains more In than near

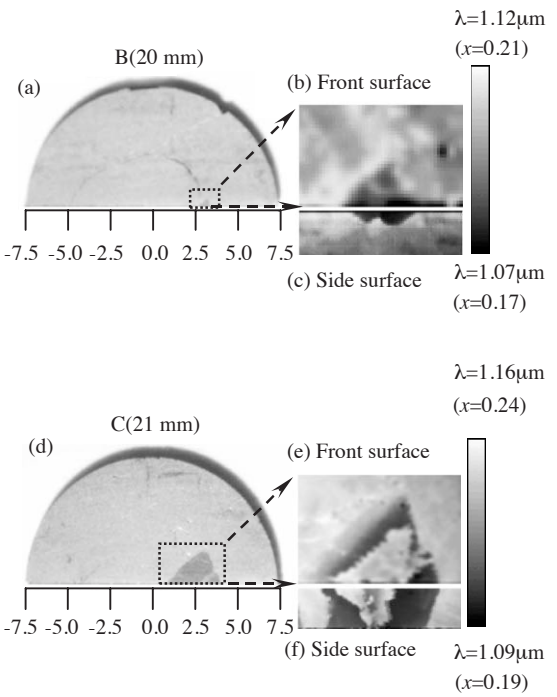

Fig. 4. 2D mapping images of PL peak wavelength measured in the wafers of B and C. The PL measurements were made in the region surrounded by dotted lines in the etching images of (a) and (d), also shown are those made at the corresponding side surfaces. The dotted lines and scales in millimeter represent the actual position of the investigated regions.

the boundary. Since the compositional inhomogeneity exists in the wafers, the measured PL peak wavelengths should have the influence of strain, which was suggested by our recent study [18].

In previous studies [7–10], several reasons for the polycrystallization mechanism in III–V semiconductor ingots were discussed. However, they only justify the initiation of polycrystallization near the peripheral region of the ingots. Since our experimental results show that the polycrystallization was initiated inside the crystal during the growth process, the causes related to the polcrystallization mechanism near the boundary of the crystal can be excluded for the crystal under investigation. As observed in our experimental results, the origin of polycrystalline region has higher Ga content compared to the surrounding. This indicates that, during the growth process, the crystallization of Ga-rich grains initiated in the melt before the growth interface was reached in this region from the seed crystal. As the growth proceeds, and the growth interface reaches the already crystallized grains, these grains get embedded in the otherwise growing single crystal, making an island of polycrystalline region. With further progress in the growth process, at every point in the growth direction in a similar manner, the polycrystalline island keeps growing before the growth interface reaches that point in the growth direction. As a result, the polycrystalline region increases in size with the growth length. We believe that these Ga-rich grains were initiated by the growth of small crystals in the solution, which could be due to supercooling or impurities in the melt, or other reasons. Originally, semiconductor melt has small kinematic viscosity compared to the thermal diffusivity, which causes local unbalance between temperature and compositional distributions. If such unbalance occurs in a saturated melt, local supercooling can easily occur compared to an unsaturated melt, which may cause polycrystallization. On the other hand, local supercooling can also occur due to gravity-induced convection [19], which may cause polycrystallization. Furthermore, constitutional supercooling originates from a diffusion layer having composition distribution in front of the growth interface, which may cause polycrystallization [20]. Since this kind of polycrystalline growth was found in a few growth experiments under the same environment, it can be comfortably assumed that this polycrystallization was not triggered by impurities. However, even in the case of impurities, the ultimate cause should be supercooling, because a higher Ga content at the origin of polycrystallization indicates supercooling. Therefore, either convection-induced local supercooling or constitutional supercooling could be the cause of polycrystalline growth in the investigated crystal.

5. Conclusions

Raman scattering and PL measurements were carried out to understand the polycrystallization mechanism in bulk $In_xGa_{1-x}As$ crystal grown by the two-step MCZM method. The etching results

indicated that a small dark region was initiated after certain growth length from the inner part of the crystal, which was then increased in size with increasing growth length. Raman results obtained in this dark region showed random change in intensity ratio LO_{GaAs}/TO_{GaAs}, which confirmed that the dark region is a polycrystalline region. Spatial variation of PL-composition map indicated the existence of drastic fluctuation of composition near the boundary as well as inside the polycrystalline region, in agreement with the Raman results. The PL map also indicated that the origin of the polycrystalline region contains more Ga than the surrounding. This may have resulted from the inhomogeneous distribution of InAs, and GaAs could be caused by local supercooling. Therefore, it can be concluded that convection-induced supercooling or constitutional supercooling could be the possible cause of polycrystallization in the crystal grown by the MCZM method.

Acknowledgements

The authors are thankful to Dr. S. Kodama for supplying a special type of sample and also to Mr. M. Suzuki for helping in PL measurements.

References

[1] W.A. Bonner, B.J. Skromme, E. Berry, H.L. Gilchirst, R.E. Nahory, in: J.S. Harris (Ed.) Proceedings of the 15th International Symposium On GaAs and Related Compounds, Atlanta, GA, 1988, Inst. Phys. Conf. Ser. 96, Inst. Phys., Bristol, 1989, pp. 337–342.
[2] K. Nakajima, T. Kusunoki, K. Otsubo, J. Crystal Growth 173 (1997) 42.
[3] Y. Nishijima, K. Nakajima, K. Otsubo, H. Ishikawa, J. Crystal Growth 197 (1999) 769.
[4] T. Suzuki, K. Nakajima, T. Kusunoki, T. Kato, J. of Electron. Mater. 25 (1996) 357.
[5] S. Kodama, Y. Furumura, K. Kinoshita, H. Kato, S. Yoda, J. Crystal Growth 208 (2000) 165.
[6] K. Kinoshita, H. Kato, M. Iwai, T. Tsuru, Y. Muramatsu, S. Yoda, J. Crystal Growth 225 (2001) 59.
[7] T.P. Chen, Y.D. Guo, T.S. Huang, L.J. Chen, J. Crystal Growth 103 (1990) 243.
[8] H.J. Koh, M.H. Choi, I.S. Park, T. Fukuda, Crystal Res. Technol. 30 (1995) 397.
[9] S. Tohono, A. Katsui, J. Crystal Growth 74 (1986) 362.
[10] W.A. Bonner, J. Crystal Growth 54 (1981) 21.
[11] M.R. Islam, P. Verma, M. Yamada, M. Tatsumi, K. Kinoshita, Jpn. J. Appl. Phys., Part 1 41 (2002) 991.
[12] M.R. Islam, P. Verma, M. Yamada, S. Kodama, Y. Hanaue, K. Kinoshita, Mater. Sci. Eng. B91–92 (2002) 66.
[13] M.R. Islam, P. Verma, M. Yamada, in: Hongjum Gao, Harald Fuchs, Dongmin Chen (Eds.), Advanced Nanomaterials and Nanodevices (Electronic book, http://www.nanotechweb.org/resources/Books), IOP Publishing Ltd., 2003, p. 912.
[14] M.R. Islam, M. Suzuki, P. Verma, M. Yamada, M. Tatsumi, Y. Hanaue, K. Kinoshita, 12th International Conference on Semiconducting and Insulating Materials, Smolenice Castle, Slovakia, IEEE Catalog No.: 02CH37343, 2002, p. 194.
[15] M. Cardona, Light Scattering in Solids, 2nd Edition, Vol. 1, Springer-Verlag, Berlin, 1983.
[16] J.P. Estrera, P.D. Stevens, R. Glosser, W.M. Duncan, Y.C. Kao, H.Y. Liu, E.A. Beam, Appl. Phys. Lett. 61 (1992) 1927.
[17] J. Groenen, G. Landa, R. Carles, P.S. Pizani, M. Gendry, J. Appl. Phys. 82 (1997) 803.
[18] M.R. Islam, M. Yamada, Conference Proceedings of Indium Phosphide and Related Materials, Santa Barbara, CA, USA, IEEE Catalog No.: 03CH37413, 2003, p. 571.
[19] Y. Hiraoka, K. Ikegami, T. Maekawa, S. Matsumoto, S. Yoda, K. Kinoshita, J. Phys. D: Appl. Phys. 33 (2000) 2508.
[20] M. Tatsumi, H. Kato, K. Kinoshita, NASDA Technical Memorandum, 2000, p. 55.